Thermo-economic assessment of flexible nuclear power plants in the UK's future low-carbon electricity system: role of thermal energy storage

Abdullah A. Al Kindi
Clean Energy Processes (CEP) Laboratory, Department of Chemical Engineering
Imperial College London, United Kingdom
e-mail: a.al-kindi18@imperial.ac.uk

Marko Aunedi
Department of Electrical and Electronic Engineering
Imperial College London, United Kingdom
e-mail: m.aunedi@imperial.ac.uk

Antonio M. Pantaleo
Department of Chemical Engineering, Imperial College London, United Kingdom
Department of Agro-Environmental Sciences, University of Bari, Italy
e-mail: a.pantaleo@imperial.ac.uk

Goran Strbac
Department of Electrical and Electronic Engineering
Imperial College London, United Kingdom
e-mail: g.strbac@imperial.ac.uk

Christos N. Markides*
Clean Energy Processes (CEP) Laboratory, Department of Chemical Engineering
Imperial College London, United Kingdom
e-mail: c.markides@imperial.ac.uk

ABSTRACT

Nuclear power plants are commonly operated as baseload units due to their low variable costs, high investment costs and limited ability to modulate their output. The increasing penetration of intermittent renewable power will require additional flexibility from conventional generation units, in order to follow the fluctuating renewable output while guaranteeing security of energy supply. In this context, coupling nuclear reactors with thermal energy storage could ensure a more continuous and efficient operation of nuclear power plants, while at other times allowing their operation to become more flexible and cost-effective. This study considers options for upgrading a 1610-MW_{el} nuclear power plant with the addition of a thermal energy storage system and secondary power generators. The analysed configuration allows the plant to generate up to 2130 MW_{el} during peak load, representing an increase of 32% in nominal rated power. The gross whole-system benefits of operating the proposed configuration are quantified over several scenarios for the UK's low-carbon electricity system. Replacing conventional with flexible nuclear plant configuration is found to generate system cost savings that are between £24.3m/yr and £88.9m/yr, with the highest benefit achieved when stored heat is fully discharged in 0.5 hours (the default case is 1 hour). At an estimated cost of added flexibility of £42.7m/yr, the proposed flexibility upgrade to a nuclear power plant appears to be economically justified for a wide range of low-carbon scenarios, provided that the number of flexible nuclear units in the system is small.

KEYWORDS

Nuclear power, power flexibility, power system optimisation, steam Rankine cycle, steam turbines, thermal energy storage.

* Corresponding author

INTRODUCTION

Nuclear power plays a significant role in achieving the ambitious global energy decarbonisation targets due to its ability to provide zero-carbon electricity [1]. Rapid cost reductions of renewables are effectively making nuclear power less economically attractive due to its increasing capital costs, long construction times, and limited and uneconomic load following capabilities of nuclear power plants. Nevertheless, nuclear power or other forms of firm low-carbon generation will be essential for ensuring energy security in a system with a high share of variable renewables. This is why the UK is still considering government-supported models for investing in nuclear power projects as part of the overall effort to achieve the target of net-zero greenhouse emissions by 2050 under the Climate Change Act [2, 3].

Nuclear power plants are commonly operated to meet baseload electricity demand because of their economic and technical characteristics. However, it is still important to investigate the potential of providing flexible and profitable nuclear power that can compete with renewables, not only in meeting baseload demand but also supplying peak demand. Jenkins et al. [4] investigated the benefits of nuclear flexibility in power system operation with a high penetration of wind and solar. The study concluded that flexible nuclear operation potentially reduces the operating costs and increases the overall reactor revenues by 2-5% compared to an inflexible nuclear reactor. The increase of revenues is mainly due to the ability of supplying day-ahead reserves and avoiding negative day-ahead electricity prices.

There are few studies that investigated the option of coupling nuclear reactors with thermal energy storage (TES) systems and secondary power generators. Carlson et al. [5] studied the thermodynamic benefits of coupling a pressurised water reactor (AP1000) with a TES system and a secondary Rankine cycle system. Three configurations based on the TES charge/discharge mechanisms and duration were investigated, and one of these configurations could provide more than 1.5 times the nominal power output. Moreover, a study of integrating nuclear power plant with a cryogenic-based energy storage technology and secondary power generation unit was performed by Li et al. [6]. The studied configuration showed the ability of generating a total net output power of 690 MW_{el} during peak times, which is 2.7 times the baseload power output of 250 MW_{el}. The two studies demonstrated the potential of flexible nuclear operation with the integration of TES unit while keeping the reactor steam output at full rated power. However, neither of these studies evaluated the economic benefits or investigated the role of flexible nuclear power in a whole-system model with a high penetration of renewables.

There is a wide range of TES technologies, which can be classified in terms of storage mechanism as: i) sensible, ii) latent, also known as phase change material (PCM), and iii) thermochemical [7]. There is a growing demand for TES, as reported in a recent study by IRENA [8] that predicts that the global market for TES could triple in size by 2030, with an increase from 234 GWh of installed capacity in 2019 to over 800 GWh within a decade. Recent research from Cardenas et al. [9] estimated the required heat storage capacity as the penetration of renewables increases, and the timescales in which energy is most efficiently stored. The paper studied the effect that the renewable penetration, allowable curtailment, storage capacity and efficiency have on the total cost of electricity in the UK scenario, concluding that the most needed flexibility service at high PV and wind energy penetration is the medium duration one, with 4 to 200 hours discharge duration.

The role of TES in systems with high renewable penetrations becomes even more prominent when considering renewable technologies such as concentrated solar power (CSP). This is evident in Gils et al. [10] paper, which analyses different European scenarios with very high

renewable penetrations and discusses the economic and technical issues. The advantages of the application of TES over batteries in combination with large-scale thermoelectric power plants were also highlighted by Ma et al. [11]. According to their analysis, the use of TES in combination with conventional power plants allows to economically support variable renewables at larger capacity and for longer discharging hours than current battery storage technologies or hydropower storage.

Decarbonisation of the electricity system will require a range of technologies to provide flexibility in the context of grid support, balancing, security of supply and integration of variable renewables [12]. These technologies will include various forms of energy storage, demand-side response, expansion of interconnection capacity and more flexible generation technologies, as well as a number of cross-vector flexibility options such as TES and power-to-X. A number of studies have shown that flexibility becomes increasingly important as carbon emissions targets for the electricity sector are reduced and therefore the provision of flexibility will become particularly critical in achieving net-zero carbon or net-negative carbon electricity supply [13].

Energy technologies linking heat and power will play a key role in the integration between heating/cooling and electricity networks, and therefore recent research has focused on the optimal design and operation of combined heat and power (CHP) systems, centralised heat pumps and TES options for district heating [14]. It has been shown in Ref. [15] that a cost-efficient supply of heat in a local district heating system may require a significantly higher volume of TES in order to help manage local grid constraints and support the integration of high penetration of variable renewables.

To adequately quantify the role of flexible solutions in future electricity systems, it is critical to model these systems with sufficient spatial-temporal resolution using a holistic system approach. The approach to system valuation of flexible nuclear configurations used in this paper is based on an extension of the whole-system modelling approach presented in Ref. [16]. This whole-system valuation approach has previously been used to assess battery storage [17], pumped-hydro storage [18] and liquid-air and pumped-heat energy storage [19].

In this paper we propose a novel approach to configuring flexible nuclear power plants and quantifying their system value in low-carbon electricity systems. More specifically, the main contributions of the paper include: 1) a technology-rich approach to configuring the design of the flexible nuclear power station based on detailed thermodynamic modelling of various individual plant components (SRC generators, steam generators, steam turbines, PCM-based thermal storage, feed pumps, condensers etc.); 2) optimisation of the thermodynamic performance of flexible nuclear plant configuration by determining efficient choices for a variety of technical parameters including the choice of PCM; 3) developing a model of flexible nuclear power plant as part of a wider high-resolution power system model; 4) quantifying the value of enhanced flexibility of nuclear generators for a range of scenarios characterised by decarbonised electricity supply and a high share of variable renewables.

METHODS

As a first step of this study, a layout is proposed for upgrading a conventional nuclear power plant with a TES system and secondary power generation cycles. Each main component of the proposed configuration is computationally modelled for thermodynamic performance evaluation. Secondly, the obtained energy performance and investment costs are used as an input for the whole-system modelling of the low-carbon electricity system in the UK, to appreciate the benefits of such flexible asset.

Power plant configuration and description

The layout of the proposed nuclear power plant, illustrated in Figure 1, consists of:

1) Nuclear power island that includes a pressurised nuclear water reactor and a steam generator (SG), which generates steam utilising nuclear thermal power.
2) Primary steam Rankine cycle (PSRC) system that contains high-pressure turbines (HPT), low-pressure turbines (LPT), a reheater (RH), a condenser, electric generators, six closed feedwater heaters (CFWH), a condensate pump, a feed pump and a deaerator.
3) TES units, indicated as TES-1 and TES-2 in Figure 1. TES-1 unit is proposed to have two PCM tanks (PCM-1 and PCM-2) connected in series. PCM-1 tank is charged using higher temperature steam flowing out from the steam generator, while PCM-2 tank is charged using steam flowing out from PCM-1 tank. Similarly, TES-2 unit has two PCM tanks (PCM-3 and PCM-4), also connected in series. However, TES-2 tanks are charged by lower temperature steam that is extracted after the HPT and before the reheater, as shown in Figure 1.
4) Two secondary power generation cycle (SSRC-1 and SSRC-2) systems. SSRC-1 is operated by discharging the heat stored in TES-1 tanks while SSRC-2 is operated by utilising the stored heat in TES-2 tanks.

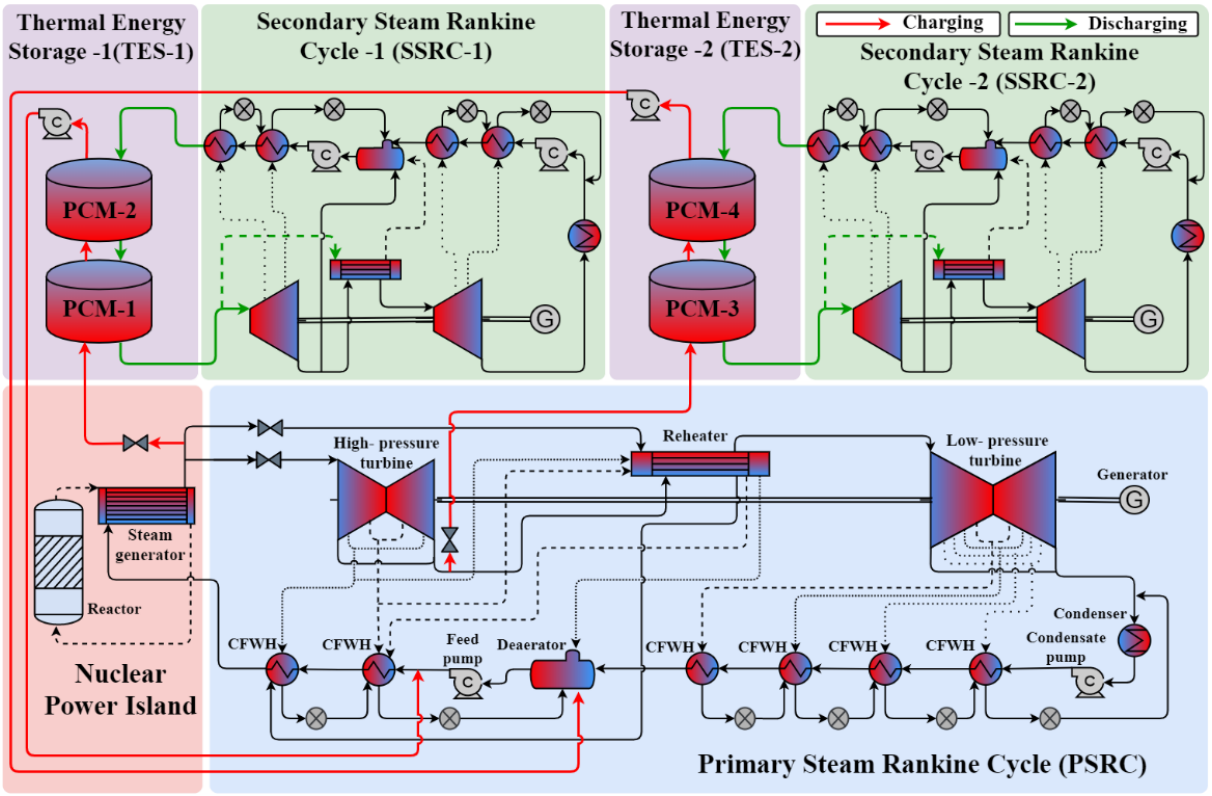

Figure 1. Layout of the proposed nuclear power plant coupled with PCM tanks as TES units and secondary power Rankine cycles (SSRCs). Red lines indicate thermal energy charging flow streams and green lines indicate thermal energy discharging flow streams.

In this study, the reactor is assumed to continuously operate at full rated thermal power whenever it is possible to avoid power disturbance in the reactor and to maximise the economic benefits of investing in such a capital-intensive energy source. In this context, most load following operations are achieved by controlling: 1) the amount of steam flowing from the steam generator to the PSRC; 2) the amount of steam directed to both TES units (i.e., charging mode); 3) the operation of both SSRCs (i.e., discharging mode).

Nuclear reactor and primary steam Rankine cycle

The selected nuclear reactor design is the European pressurised reactor (EPR), which is a pressurised water reactor that generates 4520 MW_{th} of thermal power using nuclear fission [20]. Although there is a wide range of reactor types and designs, the EPR is chosen as it is currently under construction in the UK at Hinkley Point C, and is also the choice for the potential future construction of Sizewell C [21]. It is expected that EPR design has a higher potential than other reactor designs to replace the current fleet of advanced gas-cooled reactors (AGR) in the UK due to the experience gained from constructing current EPRs. Table 1 summarises the main EPR operating parameters that are considered in the PSRC model, which is explained in detail in the next section.

Table 1. Main operation parameters of the EPR [20, 22, 23].

Parameter	Value
Reactor thermal power (MW_{th})	4520
Feedwater temperature (°C)	230
Feedwater pressure (kPa)	8300
Steam generator mass flow rate (kg/s)	2553
Steam generator outlet temperature (°C)	293
Steam generator outlet pressure (kPa)	7800

Full load operation. The full load (nominal load) of the PSRC model is formulated using the provided operation parameters and assumptions listed in Table 2. Full load operation of the PSRC means that no steam is directed to the TES units and all nuclear thermal power is utilised for electrical power generation from the PSRC generators. The enthalpy of steam exiting the nuclear-powered SG is calculated using the rate of added heat in the steam generator $\dot{Q}_{\mathrm{SG}}$ as follows:

$$\dot{Q}_{\mathrm{SG}} = \dot{m}\,(h_{\mathrm{out}} - h_{\mathrm{in}}) \tag{1}$$

Equations (2)-(5) are used to calculate the generated power by the turbines and needed by the pumps:

$$\dot{W}_{\mathrm{T}} = \dot{m}\,(h_{\mathrm{in}} - h_{\mathrm{out}}) \tag{2}$$

$$\eta_{\mathrm{T}} = \frac{(h_{\mathrm{in}} - h_{\mathrm{out}})}{(h_{\mathrm{in}} - h_{\mathrm{out,is}})} \tag{3}$$

$$\dot{W}_{\mathrm{P}} = \dot{m}\,(h_{\mathrm{out}} - h_{\mathrm{in}}) \tag{4}$$

$$\eta_{\mathrm{P}} = \frac{(h_{\mathrm{out,is}} - h_{\mathrm{in}})}{(h_{\mathrm{out}} - h_{\mathrm{in}})} \tag{5}$$

The amount of thermal power added in all CFWHs and the reheater and the outlet steam enthalpy of the deaerator are calculated using Equations (6) and (7), respectively:

$$\dot{Q}_{\mathrm{CFWH,RH}} = \dot{m}\,(h_{\mathrm{out}} - h_{\mathrm{in}}) \tag{6}$$

$$h_{\mathrm{out}} = \frac{\sum(\dot{m}h)_{\mathrm{in}}}{\sum \dot{m}_{\mathrm{in}}} \tag{7}$$

The PSRC net electrical power $\dot{W}_{\mathrm{net}}$ and the net cycle efficiency η_{PSRC} are calculated from:

$$\dot{W}_{\mathrm{net}} = (\eta_{\mathrm{Gen}} \sum \dot{W}_{\mathrm{T}}) - \sum \dot{W}_{\mathrm{P}} \tag{8}$$

$$\eta_{\mathrm{PSRC}} = \frac{\dot{W}_{\mathrm{net}}}{\dot{Q}_{\mathrm{SG}}} \tag{9}$$

Table 2. Primary steam Rankine cycle assumptions and parameters at nominal power [5, 24, 25].

Parameter	Value
Average HPT design isentropic efficiency (%)	87
Average LPT design isentropic efficiency (%)	87
Condenser pressure (kPa)	10
Pump isentropic efficiency (%)	85
Generator mechanical efficiency (%)	98
Pressure loss in the reheater (kPa)	300
Hot stream outlet steam quality in CFWHs (-)	0

One method of obtaining the operating condition of other PSRC streamlines such as the turbine side extraction pressures and mass flow rate, steam that flows from the steam generator to the reheater, etc., is to set up an optimisation model with an objective function that maximises the net cycle efficiency as in Equation (10). The model simulations are performed using MATLAB and all steam properties are obtained using REFPROP [26]. The PSRC efficiency optimisation tasks are solved using MATLAB's interior point algorithm *fmincon* or genetic algorithm function *ga.*

$$\max\{\eta_{\mathrm{PSRC}}\} \quad \dot{m}_{\mathrm{RH\ (1,2,3)}}, P_{\mathrm{HPT,SE(1,2)}}, P_{\mathrm{HPT,out}}, P_{\mathrm{LPT,SE(1,2,3,4)}}, \dot{m}_{\mathrm{HPT,SE(1,2)}}, \dot{m}_{\mathrm{LPT,SE(1,2,3,4)}} \tag{10}$$

The objective function is formulated to solve the numerical PSRC model while satisfying a set of non-linear constraints listed in Equations (11)-(14).

$$\Delta T^{\mathrm{PP}}_{\mathrm{CFWH,in}} \geq 5\ ^{\circ}\mathrm{C} \tag{11}$$

$$\Delta T^{\mathrm{PP}}_{\mathrm{CFWH,out}} \geq 5\ ^{\circ}\mathrm{C} \tag{12}$$

$$x_{\mathrm{P,in}} \leq 0 \tag{13}$$

$$T_{\mathrm{RH,out}} \geq 287\ ^{\circ}\mathrm{C} \tag{14}$$

Part-load operation (charging mode). The part-load PSRC model is constructed by considering the following off-design turbine efficiency correlation for both, the HPT and the LPT [27]:

$$\eta_{\mathrm{T}}^{\mathrm{OD}} = \eta_{\mathrm{T}}^{\mathrm{D}} - 2\left(\frac{N^{\mathrm{OD}}\sqrt{\Delta h_{\mathrm{is}}^{\mathrm{D}}}}{N^{\mathrm{D}}\sqrt{\Delta h_{\mathrm{is}}^{\mathrm{OD}}}} - 1\right)^2 \tag{15}$$

It is assumed that the shaft speed is constant for all loads as the shaft is connected to a power grid with fixed frequency, typically 50 Hz in the UK [28]. In this study, the multiple stages between the turbine inlet and the next side extraction, or between two side extractions or between the last side extraction and the main turbine outlet, are considered as one turbine stage. Therefore, the HPT turbine and the LPT are assumed to consist of 3 and 5 stages, respectively.

The part-load PSRC model also considers the change of steam pressure at the inlet and the outlet of each stage due to steam mass flow rate and temperature variations inside the turbine during part-load operation. To calculate the turbine inlet, outlet, and side extractions pressure, the following Stodola's ellipse law is applied [29, 30]:

$$\frac{\frac{\dot{m}_{\mathrm{in}}^{\mathrm{OD}}\sqrt{T_{\mathrm{in}}^{\mathrm{OD}}}}{P_{\mathrm{in}}^{\mathrm{OD}}}}{\frac{\dot{m}_{\mathrm{in}}^{\mathrm{D}}\sqrt{T_{\mathrm{in}}^{\mathrm{D}}}}{P_{\mathrm{in}}^{\mathrm{D}}}} = \frac{\sqrt{1-\left(\frac{P_{\mathrm{out}}^{\mathrm{OD}}}{P_{\mathrm{in}}^{\mathrm{OD}}}\right)^2}}{\sqrt{1-\left(\frac{P_{\mathrm{out}}^{\mathrm{D}}}{P_{\mathrm{in}}^{\mathrm{D}}}\right)^2}} \tag{16}$$

The part-load cycle efficiency expression and the adjusted optimisation objective function are:

$$\eta_{\mathrm{PSRC}}^{\mathrm{PL}} = \frac{\dot{W}_{\mathrm{net}}}{\dot{Q}_{\mathrm{SG}} - \dot{Q}_{\mathrm{TES}}} \tag{17}$$

$$\max_{\dot{m}_{\mathrm{RH\ (1,2,3)}}, \dot{m}_{\mathrm{HPT,SE(1,2)}}, \dot{m}_{\mathrm{LPT,SE(1,2,3,4)}}, \dot{m}_{\mathrm{TES-1}}, \dot{m}_{\mathrm{TES-2}}} \{\eta_{\mathrm{PSRC}}^{\mathrm{PL}}\} \tag{18}$$

The optimisation problem is solved satisfying the constraints listed in Equations (11)-(14) and the following additional constraint to reduce the impact of off-design operation on both turbines:

$$\dot{Q}_{\mathrm{TES-1}} = \dot{Q}_{\mathrm{TES-2}} \tag{19}$$

Modular TES-SSRC units (conceptual design)

A conceptual modular TES-SSRC design is proposed in this study. The modular TES-SSRC unit is designed to contain four components attached to the PSRC. These components are TES-1 (PCM-1 and PCM-2), SSRC-1, TES-2 (PCM-3 and PCM-4), and SSRC-2 as illustrated in the top side of Figure 1. The size of the modular TES-SSRC unit is determined by the amount of thermal power available for storage and the TES charging/discharging duration. One modular TES-SSRC unit is sized based on the following assumptions:

- The storage capacities of TES-1 and TES-2 are determined by calculating the amount of heat available for storage when the PSRC power output is reduced by a scale of 10% of the nominal load for 1 hour. For example, if the PSRC is operating at 50% of its nominal power for 1 hour, 5 modular TES units can be fully charged at the end of that hour.
- Both SSRC-1 and SSRC-1 are designed to fully discharge TES-1 and TES-2 in 1 hour.

TES design and phase change material selection. PCM are selected due to their ability to charge and discharge thermal power at relatively constant phase change temperatures (melting temperature) [31]. The optimal type and design (i.e., shape, dimensions, etc.) of the PCM tanks in the modular TES-SSRC system is not performed in this study. However, the selection of the PCM type is essential to determine the operation temperature range of both the SSRC-1 and SSRC-1. Table 3 summarises the calculated inlet steam conditions and the assumed outlet steam conditions of TES-1 and TES-2 as well as the nominated PCM type that suits the temperature range of the charging steam. It is also proposed that each PCM tank is designed with a specific PCM, depending on the storage temperature and the correspondent PCM melting temperature.

Table 3. Thermal properties of PCM and steam conditions of the PCM tanks [32–35]

Parameters		TES-SSRC-1		TES-SSRC-2	
		PCM-1	PCM-2	PCM-3	PCM-4
Material		$NaNO_2$	53%KNO_3+ 7%$NaNO_3$+ 40%$NaNO_2$	87%$LiNO_3$+ 13%NaCl	53%KNO_3+ 7%$NaNO_3$+ 40%$NaNO_2$
Melting temperature (°C)		282	142	208	142
Latent heat of fusion (kJ/kg)		212	110	369	110
Charging steam inlet condition	Pressure (kPa)	7800	-	2390	-
	Temperature (°C)	293	-	221	-
	Quality (-)	superheated	-	0.88	-
	Mass flow rate (kg/s)	102	102	111	111
Charging steam outlet conditions	Pressure (kPa)	-	7700	-	2290
	Temperature (°C)	-	152	-	152
	Quality (-)	-	subcooled	-	subcooled
	Mass flow rate (kg/s)	102	102	111	111

Design of SSRCs and operation (discharging mode). Discharging of stored heat is performed through SSRC-1 and SSRC-2 that are attached to TES-1 and TES-2, respectively. The temperature range of TES-2 is relatively low for steam Rankine cycles, which might not be a favourable option. However, it is still considered in this study since the size of the SSRCs is expected to be greater than 45 MW_{el}. Similarly, as in the PSRC efficiency optimisation model, the main steam parameters of the SSCRs are optimised with a set of non-linear constraints to achieve maximum cycle efficiency. The optimisation objective function of each SSRC is as follows:

$$\max\{\eta_{\mathrm{SSRC}}\} \quad P_{\mathrm{TES,in}}, \dot{m}_{\mathrm{RH}}, P_{\mathrm{HPT,SE(1,2)}}, P_{\mathrm{HPT,out}}, P_{\mathrm{LPT,SE(1,2)}}, \dot{m}_{\mathrm{HPT,SE(1,2)}}, \dot{m}_{\mathrm{DE}}, \dot{m}_{\mathrm{LPT,SE(1,2)}} \tag{20}$$

In addition to the constraints listed in Equations (11)-(14), the following constraints are applied in the SSRC optimisation model:

$$T_{\mathrm{TES,in}} \leq T_{\mathrm{m,PCM(2,4)}} - 10 \tag{21}$$

$$T_{\mathrm{TES,out}} \leq T_{\mathrm{m,PCM(1,3)}} \tag{22}$$

$$x_{\mathrm{TES,out}} \geq 1 \tag{23}$$

Moreover, the model accounts for TES heat losses to the environment as well as the impact of steam conditions variation (i.e., temperature difference, mass flow rate, pressure, etc.) on the heat transfer rate between the PCM and the steam during charging and discharging modes [36]. Therefore, a charging heat-to-heat efficiency ($\eta_{\mathrm{TES,Ch}}$) of 90% and a discharging heat-to-heat efficiency ($\eta_{\mathrm{TES,Dch}}$) of 90% are assumed. Other parameters and steam cycle assumptions are the same as for the PSRC model, as listed in Table 2.

Whole-system modelling and inputs

System assessment of flexible nuclear plants is carried out by significantly extending the whole-electricity system investment model (WeSIM), presented in Ref. [16], to include specific features of flexible nuclear generation. Capturing the interactions across various time-scales and across various asset types at sufficient temporal and spatial granularity is critical when analysing future low-carbon electricity systems. WeSIM is a whole-system analysis model that is able to simultaneously optimise long-term investments into generation, network and storage assets, and short-term operation decisions in order to satisfy the demand at least cost while ensuring adequate security of supply, sufficient volumes of ancillary services and meeting system-wide carbon emission targets [16]. WeSIM can quantify trade-offs between using various sources of flexibility, such as demand-side response (DSR) and energy storage, for real-time balancing and for management of network constraints. A detailed formulation of the model has been previously provided in Ref. [16]; therefore, only the new elements of the model formulation that are relevant for flexible nuclear power plant modelling are presented here. Extensions to the WeSIM model presented here have been implemented in FICO Xpress Optimisation framework [37].

Mathematical formulation of the whole-system model. The formulation of the system model presented here assumes a single-node system without considering any distribution, transmission or interconnection assets. A shortened form of the objective function for the mixed-integer linear problem is given in Equation (24). The model minimises the total system cost, which is the sum of annualised investment cost associated with power generation (G), flexible nuclear (N), electrolyser (E), hydrogen storage (H) and battery storage (S) assets, and the annual operating cost across all time intervals considered in the study (in this case all 8760 hours of a year). Component investment costs are expressed as products of per-unit cost parameters (π) and decision variables for total capacity (μ). The operating cost term (C) is the function of

generation output decision variables (p) and reflects the variable operating costs, no-load costs and start-up costs of thermal generators.

$$\min\{z\} = \sum_{i=1}^{G} \pi_i^G \mu_i^G + \sum_{i=1}^{N} \pi_i^N \mu_i^N + \sum_{i=1}^{E} \pi_i^E \mu_i^E + \sum_{i=1}^{H} \pi_i^H \mu_i^H + \sum_{i=1}^{S} \pi_i^S \mu_i^S + \sum_{t=1}^{\tau} \left(\sum_{i=1}^{G} C_{i,t}^G(p_{i,t}^G) + \sum_{i=1}^{N} C_{i,t}^N(p_{i,t}^N) \right) \quad (24)$$

A number of further constraints are formulated in the model (details can be found in Ref. [16]):

- Power supply-balance constraints.
- Operating reserve constraints for fast and slow reserves.
- Generator operating constraints, including minimum and maximum output, ramping constraints and minimum up and down time constraints.
- Annual load factor constraints to account for planned maintenance.
- Available energy profiles for variable renewables.
- Demand-side response constraints that allow demand shifting.
- Emission constraints to limit total annual carbon emissions from the electricity system.
- Security of supply constraints.

The number of flexible nuclear units in the system is denoted by n_{FN}, which can be either specified as fixed input or optimised by the model. Unit commitment variables u are formulated for each time interval t and separately for the PSRC and SSRC components of the flexible nuclear units:

$$u_{\mathrm{PSRC},t}, u_{\mathrm{SSRC},t} \leq n_{\mathrm{FN}} \quad (25)$$

In all studies, the PSRC is assumed to operate as a must-run generator, i.e., that all PSRC units are always in synchronised operation (although not necessarily at full output).

The aggregate heat output of flexible nuclear units' steam generators $\dot{Q}_{\mathrm{SG},t}$ is bounded from below and above by the product of n_{FN} and the lower and upper bound per one unit:

$$n_{\mathrm{FN}} \cdot \dot{Q}_{\mathrm{SG}}^{\min} \leq \dot{Q}_{\mathrm{SG},t} \leq n_{\mathrm{FN}} \cdot \dot{Q}_{\mathrm{SG}}^{\max} \quad (26)$$

Aggregate power output of PSRC and SSRC components is bounded by the relevant minimum and maximum output levels when these generators are operating:

$$u_{\mathrm{PSRC},t} \cdot \dot{W}_{\mathrm{PSRC}}^{\min} \leq \dot{W}_{\mathrm{PSRC},t} \leq u_{\mathrm{PSRC},t} \cdot \dot{W}_{\mathrm{PSRC}}^{\max} \quad (27)$$

$$u_{\mathrm{SSRC},t} \cdot \dot{W}_{\mathrm{SSRC}}^{\min} \leq \dot{W}_{\mathrm{SSRC},t} \leq u_{\mathrm{SSRC},t} \cdot \dot{W}_{\mathrm{SSRC}}^{\max} \quad (28)$$

Note that the multiple modules of TES-SSRC units discussed in the previous section are treated aggregately in this formulation. The rates of charging and discharging heat into/from heat storage are given by:

$$\dot{Q}_{\mathrm{TES,Ch},t} \leq n_{\mathrm{FN}} \cdot \dot{Q}_{\mathrm{TES,Ch}}^{\max} \quad (29)$$

$$\dot{Q}_{\mathrm{TES,Dch},t} \leq n_{\mathrm{FN}} \cdot \dot{Q}_{\mathrm{TES,Dch}}^{\max} \quad (30)$$

The energy content of TES is limited by the aggregate storage size, while the TES balance equation accounts for charging and discharging heat subject to losses:

$$Q_{\mathrm{TES},t} \leq n_{\mathrm{FN}} \cdot Q_{\mathrm{TES}}^{\max} \quad (31)$$

$$Q_{\mathrm{TES},t} = Q_{\mathrm{TES},t-1} + \left(\eta_{\mathrm{TES,Ch}} \, \dot{Q}_{\mathrm{TES,Ch},t} - \frac{1}{\eta_{\mathrm{TES,Dch}}} \dot{Q}_{\mathrm{TES,Dch},t} \right) \cdot \delta \quad (32)$$

Heat balance constraints are formulated to ensure that the heat produced by steam generator is used either directly in the PSRC unit or partially stored in TES, while any heat released from TES is used to power the SSRC unit:

$$\dot{Q}_{\mathrm{SG},t} - \dot{Q}_{\mathrm{TES,Ch},t} = \dot{Q}_{\mathrm{PSRC},t} = \beta_{\mathrm{PSRC}} \cdot u_{\mathrm{PSRC},t} + \gamma_{\mathrm{PSRC}} \cdot \dot{W}_{\mathrm{PSRC},t} \quad (33)$$

$$\dot{Q}_{\mathrm{TES,Dch},t} = \dot{Q}_{\mathrm{SSRC},t} = \beta_{\mathrm{SSRC}} \cdot u_{\mathrm{SSRC},t} + \gamma_{\mathrm{SSRC}} \cdot \dot{W}_{\mathrm{SSRC},t} \quad (34)$$

The link between the input heat and output electricity for PSRC and SSRC units in Equations (33) and (34) is formulated by assuming a no-load heat rate β that is incurred whenever the unit is operating regardless of the output level, and incremental heat rate γ that multiplies the generator output level. These heat rate parameters are estimated from the results of thermodynamic modelling presented earlier in this section. Other operating constraints such as ramping and minimum up/down times were also implemented in the model but are omitted here for brevity.

Finally, the annual availability constraint for the steam generator output is formulated based on the product of the annual availability factor α_{FN} and the duration of the year in hours τ:

$$\sum_{t=1}^{\tau} \dot{Q}_{\mathrm{SG},t} \leq n_{\mathrm{FN}} \cdot \dot{Q}_{\mathrm{SG}}^{\max} \cdot \tau \cdot \alpha_{\mathrm{FN}} \quad (35)$$

The total operation cost of flexible nuclear units contributing to total system cost in Equation (24) is simply equal to the product of total SG output and the cost of nuclear fuel.

Assessing the value of flexible nuclear units in low-carbon electricity systems. System value of flexible nuclear generation in this paper has been quantified as a *gross system benefit* from replacing a standard nuclear unit with a flexible alternative that also includes TES and SSRC generation. In the first step, we ran the whole-system model to minimise the total system cost and construct a series of *counterfactual* scenarios in which nuclear generation had no added flexibility features. In the second step, a series of model runs was performed with nuclear units being replaced with flexible nuclear configurations that included TES and SSRC generation. Any resulting reduction in total system cost (but not reflecting the cost of making the nuclear generation more flexible) is then interpreted as gross system benefit of flexible nuclear.

Gross system benefit of flexible nuclear is a useful benchmark to compare against the estimated cost of delivering increased flexibility through TES and a secondary steam cycle. This comparison is provided in the results section, with the aim of identifying those electricity system features that result in a positive net benefit of flexible nuclear generation.

Scenarios used for assessing the value of flexible nuclear generation. In order to examine the key drivers for the system value of flexible nuclear, a number of scenarios have been run for different inputs assumptions. Two generic systems have been assumed, North and South, both sized to approximately match the GB electricity system. Although the annual demand volume in both systems was the same, around 400 TWh, the North system had a higher share of electrified heating demand then South, but a lower share of cooling demand. Also, in the North system it was assumed that onshore and offshore wind were available at relatively higher capacity factors (40% and 54%, respectively), while for solar PV the capacity factor was only 14%. In contrast, in the South the assumed PV capacity factor was 24%, while wind capacity factors were lower than in the North (35% and 49% for onshore and offshore, respectively).

In all case studies except one it was assumed that there is exactly one nuclear unit in the system, with the PSRC rating of 1610 MW_{el}. This unit was assumed to be either conventional (in the counterfactual studies) or equipped with TES and SSRC units in the flexible studies.

For each of the two systems (North and South) a series of scenarios was investigated, as listed in Table 4, by running both counterfactual and flexible nuclear studies. The purpose of these scenarios was to explore the impact of various assumptions on the system benefit of flexible nuclear, including the level of system carbon emissions, number of nuclear units in the system, variations in SSRC duration (ratio between TES size and maximum SSRC heat intake; default assumption was 1 hour), uptake and cost of battery storage and DSR, and the ability to invest in carbon offsets such as Bioenergy with Carbon Capture and Storage (BECCS).

Table 4. List of system scenarios used for quantifying system benefits of flexible nuclear.

ID	Scenario description
A	Net zero carbon system
B	Carbon intensity target of 25 gCO_2/kWh
C	Carbon intensity target of 50 gCO_2/kWh
D	5 nuclear units instead of one
E1	SSRC duration of 0.5 hours
E2	SSRC duration of 2 hours
E3	SSRC duration of 4 hours
F	Higher cost of battery storage (50% higher than baseline)
G	Low DSR uptake of 25% (vs. 50% used in other cases)
H	No investment in carbon offsets (BECCS)

RESULTS AND DISCUSSION

Performance of the primary power generation cycle (PSRC)

The main operating parameters of the PSRC that resulted in maximum cycle efficiency at nominal power are listed in Table 5. The calculated steam generator outlet temperature is 294 °C at 7800 kPa, which represents a slightly superheated steam. The steam enters the HPT at the same conditions and expands to 2390 kPa, reheated to 289 °C in the reheater, and then continue expanding to a condensing pressure of 10 kPa. The calculated net electrical power is 1610 MW_{el}, which is 1.2% less than the declared design net capacity of 1630 MW_{el} of EPR [20]. Such difference is expected since the actual EPR steam cycle parameters and components might be different to what is assumed in this study. The obtained maximum PSRC heat-to-electricity efficiency is 36%, which is equivalent to a heat rate of 10.1 GJ/MWh_{el}. This efficiency is relatively high compared to other pressurised light water reactor designs (an average of 33%) but it is achievable with recent improvements in component efficiencies [38].

Table 5. Obtained PSRC steam parameters at nominal power.

Parameter	Value
HPT main outlet pressure (kPa)	2390
HPT main outlet temperature (°C)	221
Reheater main inlet mass flow rate (kg/s)	1880
Reheater outlet temperature (°C)	289
LPT main outlet pressure (kPa)	10
LPT main outlet mass flow rate (kg/s)	1370
Condensate pump outlet pressure (kPa)	2390
Net electrical power (MW_{el})	1610
Cycle efficiency (%)	35.7

PSRC performance during part-load operation (TES charging mode). The nominal operating conditions (i.e., design isentropic efficiencies, mass flow rate, pressure, and temperature of both turbines) of the PSRC are extracted to run the part-load PSRC model using Equations (15) and (16). Figure 2 presents the maximum obtained cycle efficiencies, as defined in Equations (9) and (17), from 50% to 100% of nominal power (i.e., from 806 to 1610 MW_{el}).

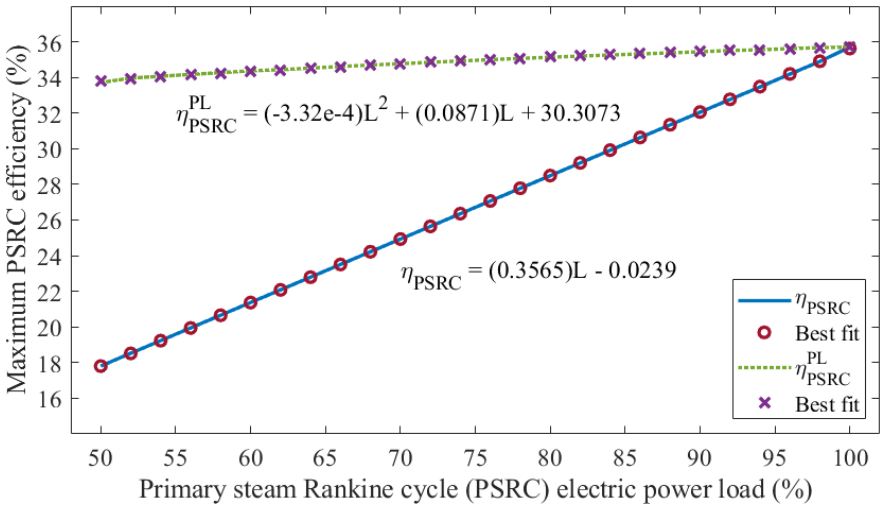

Figure 2. Maximum PSRC efficiency for electric loads from 50% to 100% of nominal power.

The PSRC efficiency ranges from 18% at 50% power load to 36% at 100% power load. The trend is linear since the rate of heat addition is constant for all power loads (i.e., reactor is operating at maximum thermal power level). However, the part-load PSRC efficiency is higher for all loads, ranging from 34% at 50% power load to 36% at maximum load. The difference is less than 2% and mainly due to the decrease of turbine isentropic efficiency at part-load operations. Moreover, best fit lines are constructed for both PSRC efficiency indicators in order to allow estimating the PSRC efficiency and the incremental heat rate required by the whole-system model.

TES-SSRC modular unit thermodynamic performance

The calculated average amount of stored heat in each TES-SSRC module is 195 MWh_{th} for both TES-1 and TES-2 tanks. This is calculated from charging thermal power of 217 MW_{th} lasting 1 hour and the assumed 90% heat-to-heat charging efficiency for TES-1 and TES-2. In this study, it is assumed that 5 TES-SSRC modules are installed. Therefore, the calculated total amount of stored heat in the 5 modules is 1950 MWh_{th}.

Results obtained from the efficiency optimisation model of SSRC-1 and SSRC-2 are summarised in Table 6. The steam inlet temperature is 132 °C for both cycles. However, the boiling (i.e., saturation) steam pressure at the TES inlet is higher for SSRC-1 since steam is boiled at a temperature of 272 °C, which is 10 °C below the melting temperature of PCM-1. For SSRC-2, the maximum temperature is 208 °C and steam is boiled at 198 °C (saturation pressure of 1490 kPa). SSRC-1 delivers 57.6 MW_{el} of net electric power, resulting in a cycle efficiency of 30%, while SSRC-2 generates 46.3 MW_{el} of electric power at 24% of cycle efficiency. Although the SSRC-2 efficiency is relatively high, it operates at low pressure and temperature range that is not recommended for steam Rankine cycles. Thus, other working fluids such as organic fluid will be considered and compared with steam in future research. The total amount of electrical power from one TES-SSRC module is 104 MW_{el}, which results in 520 MW_{el} output if all 5 installed modules are simultaneously discharging at full power. Hence, the maximum

power output of the proposed configuration is 2130 MW_{el} (1610 MW_{el} from PSRC and 520 MW_{el} from the SSRCs), which is 32% higher than the nominal PSRC power output.

Table 6. Main SSRC-1 and SSRC-2 operating parameters for 1 hour discharging duration.

Parameter	SSRC-1	SSRC-2
TES discharging thermal power (MW_{th})	195	195
TES steam inlet temperature (°C)	132	132
TES steam outlet temperature (°C)	282	208
TES steam mass flow rate (kg/s)	77.2	77.5
TES steam inlet pressure (kPa)	5680	1490
Condensing pressure (kPa)	10	10
Reheater outlet temperature (°C)	277	203
Net electrical power (MW_{el})	57.6	46.3
Cycle efficiency (%)	29.6	23.7

Benefits of flexible nuclear in low-carbon electricity systems

The results of gross system benefit assessment of flexible nuclear across the two systems considered in this study are shown in Figure 3 (A) for the North system and (B) for South system. The two systems are characterised by different shares of wind and solar PV generation and different seasonal demand variations. The system benefits represent annualised system cost savings across different scenarios, based on annualised values for asset investment costs and annual operating costs. For all cases, system benefits are broken down into various cost components, including generation investment, operating cost (OPEX), storage investment, electrolyser investment and hydrogen storage investment. Note that the system benefits are always expressed per one flexible nuclear unit (with a PSRC size of 1610 MW_{el}), so that in Scenario D with 5 flexible nuclear units the total system benefit was divided by 5. These benefits can be compared to the costs required to achieve the enhanced flexibility, i.e., the additional investment cost of TES and SSRC modules.

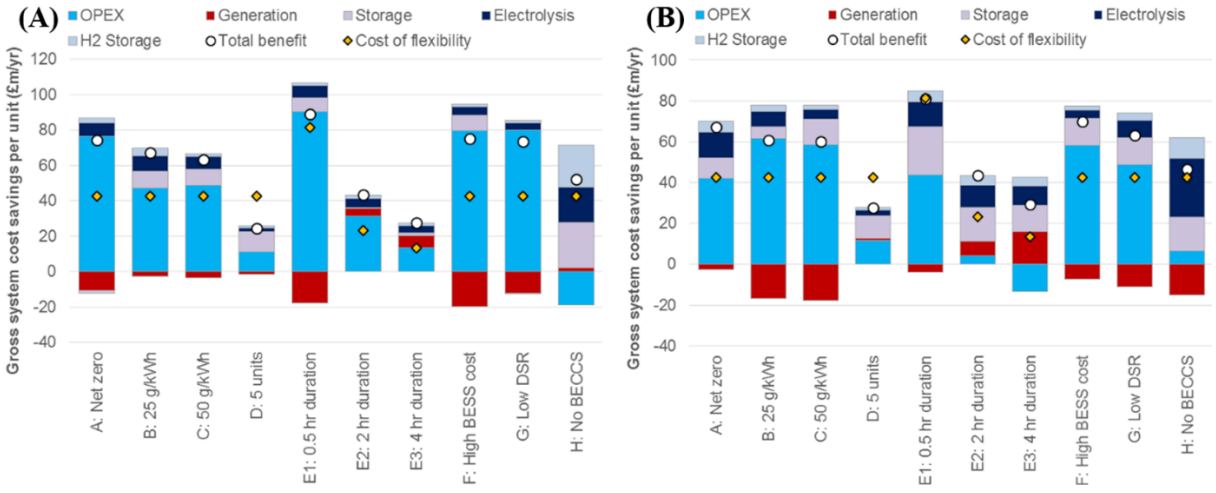

Figure 3. Gross system benefit of flexible nuclear across scenarios (A) in the North system and (B) in the South system. Different components in stacked column charts represent changes in different system cost categories. White dots represent total system benefits, while orange dots represent estimated costs of enhanced flexibility from nuclear plants, due to the related investment costs.

The key conclusions from the above results are as follows:

- System benefit of flexible nuclear generally consists of multiple components, indicating that the enhanced flexibility of nuclear generators can displace alternative flexibility options such as battery and hydrogen storage with electrolysers, as well as the investment and operating cost of generation capacity. The compound benefit of nuclear flexibility can sometimes have negative components (e.g., the generation component) due to the reconfiguration of the rest of the generation mix and changes in its output, but those are more than offset by positive cost savings in other components.
- The benefit increases with more stringent carbon emission targets, from £60.1-63.1m/yr with 50 gCO_2/kWh to £67.4-74.3m/yr for a net-zero carbon system.
- System values observed in the North system tend to be slightly higher than in the South system if the TES-SSRC duration is 1 hour. This can be explained by the higher PV and lower wind penetration in the South, and the need for longer-term flexibility (i.e., over multiple hours) to compensate for the variability of PV generation when compared to wind. For the same reason, a higher system value is observed in the South system with 4-hour duration of the TES-SSRC unit.
- System benefits diminish with a larger number of nuclear units, so that with 5 flexible units the benefit per one unit is only about a third of the benefit achieved by a single unit.
- Increasing the power-to-energy ratio of SSRC generators for the same TES size results in significantly higher system benefits, and vice versa, but on the other side also increases the cost of the flexible nuclear assets.
- Increasing the cost of battery storage (BESS) results in a marginally higher benefit of flexible nuclear (£75.1m/yr in the North and £69.9m/yr in the South), while reducing the uptake of DSR does not appear to have a material impact on the system value of flexible nuclear.
- Preventing the model to invest into BECCS carbon offsets tends to reduce the system value of flexible nuclear, which now has to compete with biomass and hydrogen generation in the counterfactual case, rather than with CCS and CCGT generation combined with carbon offsets.

Also added to charts in Figure 3 is the comparison of system gross value with an estimate of the investment cost of enhanced flexibility. Orange dots in the charts represent the estimated cost values based on the average cost of TES of £25/kWh_{th} and the cost of SSRC of £965/kW_{el} [39, 40]. With these assumptions the annualised cost of added flexibility is estimated at £42.7m/yr per one unit with the default duration assumption for the TES-SSRC component of 1 hour. This cost increases to £81.5m/yr for 0.5-hour duration and drops to £23.3m/yr and £13.5m/yr for 2-hour and 4-hour durations, respectively. At these cost estimates the flexibility upgrade appears to be cost-efficient (i.e., its benefits exceeding the cost) in all cases except with 5 units added to the system instead of one. The highest net benefit (i.e., the difference between gross benefit and cost) is observed in the net zero and high BESS cases, at £31.6-32.4m/yr in the North system and £24.7-27.3m/yr in the South system.

Finally, Figure 4 illustrates how individual components of a flexible nuclear plant are utilised on an hourly basis. The example shown in Figure 4 represents a winter week in the North system, and includes hourly profiles for SG heat output, power output from PSRC and SSRC, and net heat output from TES (difference between discharging and charging). To help identify key drivers for the operating patterns of flexible nuclear, the chart also presents the level of net demand in the system, which is obtained as the difference between total system demand (before any DSR or battery storage actions) and total variable renewable output, which included onshore and offshore wind and solar PV generation.

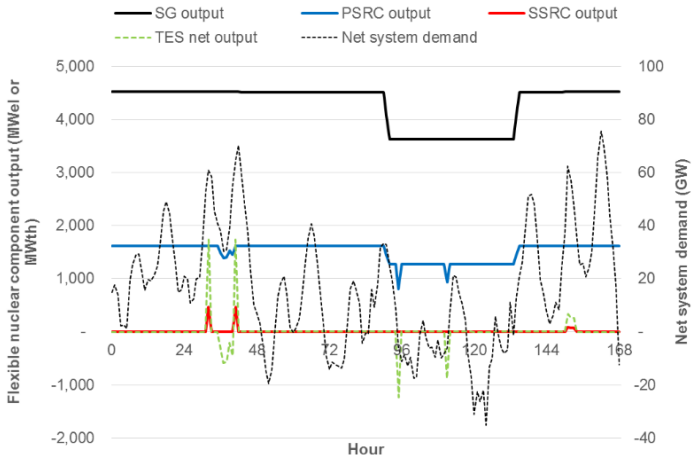

Figure 4. Hourly operation of flexible nuclear generation during a winter week in North system. Net system demand represents the difference between system demand and total wind and PV output, and is plotted against the right-hand axis.

As expected, the SSRC generation is activated only during periods of high net demand (i.e., during periods of low renewable output) when energy in the system is scarce, which in the example shown in Figure 4 occurs on the second and seventh day of the week. Note that SSRC generator is not always operating during high net demand conditions given that there are other forms of flexibility (DSR and battery storage) with time-varying availability that are also optimised by the model. Heat stored in TES units is replenished during periods of relatively lower net demand, which is observed at midday on Day 2, and around midnight and midday on Day 5. Also note that during Days 5 and 6 the supply of renewable electricity is so abundant that it results in very low or even negative net demand. The SG output on those days is therefore adjusted downwards by 20% (corresponding to the lowest allowed operating point), and so is the PSRC output, which is further reduced down to 50% of nominal output during those hours when heat is stored into TES units.

CONCLUSION

A thermodynamic analysis of an upgraded nuclear power plant coupled with thermal energy storage and secondary power generators was presented. It also quantifies the benefits of operating this flexible nuclear power plant in a low-carbon electricity system approximating the UK system. The thermodynamic modelling and primary power generation cycle efficiency optimisation framework presented here allow for identifying the optimal operating conditions during nominal load and part-load operations, as well as determining the technical design constraints of the proposed modular TES-SSRC units. The proposed whole-system electricity model enables quantifying the system value of enhanced flexibility of such nuclear generators in the context of decarbonising the electricity supply with a high share of variable renewables.

Performance predictions show that the proposed configuration could increase its overall power output during peak load by 32% of its nominal rated power, from 1610 MW_{el} to 2130 MW_{el}, with an overall electric-to-electric roundtrip efficiency of 64%. The peak power output could be increased in cases where additional TES-SSRC modules are installed (i.e., more than 5) or when the SSRC generators are sized with a higher power-to-energy ratio utilising the current TES capacity. The gross system economic benefit of a flexible nuclear unit such as that considered in the paper was quantified as reduction in total system cost resulting from replacing conventional with flexible nuclear plant, and was found to be up to about £75m/yr in the majority of the analysed

scenarios. This equates to almost £1bn in capitalised benefit of flexibility. Nevertheless, the value was found to vary considerably with system characteristics such as the composition of the low-carbon generation mix, carbon target, level of flexibility, and plant parameters such as SSRC duration. This clearly suggests that the value of this technology will be system-dependent, and therefore system characteristics should be adequately considered when evaluating the benefits of different flexible nuclear plant configurations and choosing the most cost-efficient design.

Future work related to the proposed flexible nuclear power plant configuration includes investigation of other technically applicable steam extraction points from the PSRC for charging the TES system, consideration of different working fluids for the secondary power generation cycle, detailed sizing of PCM tanks, thermodynamic analysis of charging and discharging the TES, and cost-optimisation of the size of individual components from the system perspective.

ACKNOWLEDGMENT

This work was supported by the UK Engineering and Physical Sciences Research Council (EPSRC) [grant number EP/R045518/1]. Data supporting this publication can be obtained on request from cep-lab@imperial.ac.uk.

NOMENCLATURE

Subscripts/superscripts

Ch	charging	net	net
D	design point	OD	off-design point
Dch	discharging	out	outlet
DE	deaerator	P	pump
FN	flexible nuclear	PL	part-load
Gen	generator	pp	pinch-point
HPT	high-pressure turbine	PSRC	primary steam Rankine cycle
in	inlet	RH	reheater
is	isentropic	SE	side extraction
LPT	low-pressure turbine	SG	steam generator
m	melting	SSRC	secondary steam Rankine cycle
max	maximum	T	turbine
min	minimum	TES	thermal energy storage

Greek symbols

α	availability factor (-)	η	efficiency (%)
β	no-load heat rate (MWh_{th}/hour)	μ	total capacity (W)
γ	incremental heat rate (MW_{th}/ MW_{el})	π	per-unit cost (£/W/yr)
δ	duration of unit time interval (hours)	τ	number of time intervals (hours)
Δ	difference (-)		

Symbols

C	operating cost function (£)	Q	heat (J)
E	number of electrolyser assets (-)	$\dot{Q}$	rate of heat (W)
G	number of power generation assets (-)	S	number of battery storage assets (-)
h	enthalpy (J/kg)	t	time interval (hours)
H	number of hydrogen storage assets (-)	T	temperature (K)
$\dot{m}$	mass flow rate (kg/s)	u	unit commitment (-)
n	number (-)	$\dot{W}$	power (W)
N	number of flexible nuclear assets (-)	x	steam quality (-)
P	pressure (Pa)	z	total system cost (£)

REFERENCES

1. International Atomic Energy Agency (IAEA), Climate Change and Nuclear Power, 2020.
2. Department of Business, Energy & Industrial Strategy, Nuclear Industrial Strategy - The UK ’s Nuclear Future, 2013.
3. Department of Business, Energy & Industrial Strategy, Climate Change Act 2008 (2050 Target Amendment) Order 2019, https://www.legislation.gov.uk/uksi/2019/1056 [Accessed: 13-Apr-2021]
4. Jenkins, J. D., Zhou, Z., Ponciroli, R., Vilim, R. B., et al., The benefits of nuclear flexibility in power system operations with renewable energy, *Applied Energy*, Vol. 222, pp 872-884, 2018.
5. Carlson, F. and Davidson, J. H., Parametric study of thermodynamic and cost performance of thermal energy storage coupled with nuclear power, *Energy Conversion and Management*, Vol. 236, article no: 114054, 2021.
6. Li, Y., Cao, H., Wang, S., Jin, Y., et al., Load shifting of nuclear power plants using cryogenic energy storage technology, *Applied Energy*, Vol. 113, pp 1710-1716, 2014.
7. Herrmann, U. and Kearney, D. W., Survey of thermal energy storage for parabolic trough power plants, *Journal of Solar Energy Engineering*, Vol. 124, pp 145-152, 2002.
8. International Renewable Energy Agency (IRENA), Innovation Outlook: Thermal Energy Storage, 2020.
9. Cárdenas, B., Swinfen-Styles, L., Rouse, J., Hoskin, A., et al., Energy storage capacity vs. renewable penetration: A study for the UK, *Renewable Energy*, Vol. 171, pp 849-867, 2021.
10. Gils, H. C., Scholz, Y., Pregger, T., Luca de Tena, D. and Heide, D., Integrated modelling of variable renewable energy-based power supply in Europe, *Energy*, Vol. 123, pp 173-188, 2017.
11. Ma, Z., Davenport, P. and Zhang, R., Design analysis of a particle-based thermal energy storage system for concentrating solar power or grid energy storage, *Journal of Energy Storage*, Vol. 29, article no: 101382, 2020.
12. Strbac, G., Pudjianto, D., Aunedi, M., Djapic, P., et al., Role and value of flexibility in facilitating cost-effective energy system decarbonisation, *Progress in Energy*, 2, 2020.
13. Aunedi, M., Wills, K., Green, T. and Strbac, G., Net-zero GB electricity: cost-optimal generation and storage mix, *Energy Futures Lab White Paper*, 2021, https://www.imperial.ac.uk/energy-futures-lab/reports/white-papers/net-zero-gb-electricity/ [Accessed: 06-Jul-2021]
14. Hast, A., Rinne, S., Syri, S. and Kiviluoma, J., The role of heat storages in facilitating the adaptation of district heating systems to large amount of variable renewable electricity, *Energy*, Vol. 137, pp 775-788, 2017.
15. Aunedi, M., Pantaleo, A. M., Kuriyan, K., Strbac, G. and Shah, N., Modelling of national and local interactions between heat and electricity networks in low-carbon energy systems, *Applied Energy*, Vol. 276, article no: 115522, 2020.
16. Pudjianto, D., Aunedi, M., Djapic, P. and Strbac, G., Whole-system assessment of value of energy storage in low-carbon electricity systems, *IEEE Transactions on Smart Grid*, Vol. 5, No. 2, pp 1098–1109, 2014.
17. Strbac, G., Aunedi, M., Konstantelos, I., Moreira, R., et al., Opportunities for energy storage: Assessing whole-system economic benefits of energy storage in future electricity systems, *IEEE Power and Energy Magazine*, Vol. 15, pp 32-41, 2017.
18. Teng, F., Pudjianto, D., Aunedi, M. and Strbac, G., Assessment of future whole-system value of large-scale pumped storage plants in Europe, *Energies*, Vol. 11, article no: 246, 2018.
19. Georgiou, S., Aunedi, M., Strbac, G. and Markides, C. N., On the value of liquid-air and pumped-thermal electricity storage systems in low-carbon electricity systems, *Energy*, Vol. 193, article no: 116680, 2020.
20. International Atomic Energy Agency (IAEA), Country Statistics, Hinkley Point C-1, 2021,

https://pris.iaea.org/PRIS/CountryStatistics/ReactorDetails.aspx?current=1072 [Accessed: 27-Mar-2021]
21. Electric de France Energy (EDF), Nuclear New Build Projects, 2021, https:// www.edfenergy.com/ energy/nuclear-new-build-projects [Accessed: 27-Mar-2021]
22. AREVA, European Pressurised Reactor, 2005, http://www.ftj.agh.edu.pl/~cetnar/epr/EPR-broszura.pdf [Accessed: 27-Mar-2021]
23. AREVA Nuclear Power and Electric de France Energy (EDF), UK-EPR, Fundamental Safety Overview, Chapter A: EPR Design Description, 2007.
24. Fröhling, W., Unger, H. M. and Dong, Y., Thermodynamic assessment of plant efficiencies for HTR power conversion systems, International Atomic Energy Agency (IAEA), 2002.
25. Wibisono, A. F. and Shwageraus, E., Thermodynamic performance of pressurized water reactor power conversion cycle combined with fossil-fuel superheater, *Energy*, Vol. 117, pp 190-197, 2016.
26. Lemmon, E.W., Bell, I.H., Huber, M.L. and McLinden, M.O., NIST Standard Reference Database 23: Reference Fluid Thermodynamic and Transport Properties-REFPROP, Version 10.0, National Institute of Standards and Technology, 2018.
27. Grote W., Ein Beitrag zur modellbasierten regelung von entnahmedampfturbinen. *Ph.D. Dissertation*, Ruhr-Universität, Bochum, 2009.
28. Gundogdu, B., Nejad, S., Gladwin, D. T. and Foster, D. A., A battery energy management strategy for U.K. enhanced frequency response and triad avoidance, *IEEE 26th International Symposium on Industrial Electronics (ISIE)*, pp 26-31,2017.
29. Cooke, D. H., On prediction of off-design multistage turbine pressures by Stodola's ellipse, *Journal of Engineering for Gas Turbines and Power*, Vol. 107, pp 596-606, 1984.
30. Fuls, W. F., Enhancement to the traditional Ellipse Law for more accurate modeling of a turbine with a finite number of stages, *Journal of Engineering for Gas Turbines and Power*, Vol. 139, article no: 112603, 2017.
31. Dirker, J., Juggurnath, D., Kaya, A., Osowade E. A., et al., Thermal energy processes in direct steam generation solar systems: Boiling, condensation and energy storage – A review, *Frontiers in Energy Research*, Vol. 6, article no: 147, 2019.
32. Sarbu, I. and Dorca, A., Review on heat transfer analysis in thermal energy storage using latent heat storage systems and phase change materials, *International Journal of Energy Research*, Vol. 43, pp 29-64, 2019.
33. Wei, G., Wang, G., Xu, C., Ju, X., et al., Selection principles and thermophysical properties of high temperature phase change materials for thermal energy storage: A review. *Renewable and Sustainable Energy Reviews*, Vol. 81, pp 1771-1786, 2018.
34. Bauer, T., Steinmann, W., Laing, D. and Tamme, R., Thermal energy storage materials and systems, *Annual Review of Heat Transfer*, Vol. 15, pp 131-177, 2012.
35. Fernández, A. G., Galleguillos, H., Fuentealba, E. and Pérez, F. J., Thermal characterization of HITEC molten salt for energy storage in solar linear concentrated technology, *Journal of Thermal Analysis and Calorimetry*, Vol. 122, pp 3-9, 2015.
36. Li, P., Van Lew, J., Chan, C., Karaki, W., et al., Similarity and generalized analysis of efficiencies of thermal energy storage systems, *Renewable Energy*, Vol. 39, pp 388-402, 2012.
37. Fico Xpress Optimization, https://www.fico.com/en/products/fico-xpress-optimization [Accessed: 14-May-2021]
38. Breeze P., *Power Generation Technologies*, Second edition, Newnes, London, 2019.
39. Sarbu, I. and Sebarchievici, C., A Comprehensive review of thermal energy storage, *Sustainability*, Vol. 10, No. 1, article no: 191, 2018.
40. National Renewable Energy Laboratory (NREL), System Advisor Model (SAM), https://sam.nrel.gov [Accessed: 12-Feb-2021]